Original articles

Research article
https://doi.org/10.17308/kcmf.2024.26/11817

Electrochemical impedance of porous tantalum solids: modeling of frequency response

A. V. Syugaev✉, V. E. Porsev

¹Udmurt Federal Research Centre of the Ural Branch of the Russian Academy of Sciences
34 Tatyana Baramzina str., Izhevsk 426067, Russian Federation

Abstract

The paper proposes a new approach to the analysis of electrochemical impedance spectra of porous tantalum bodies, which involves modeling the frequency response via an equivalent circuit that takes into account the pore hierarchy. It was shown that the proposed circuit describes well the experimental data and allows characterization of the porous structure, including the contribution of different types of pores to the total capacitance of the porous body, characteristic relaxation times, and activation frequencies for different type pores. Two types of samples were analyzed: a porous tantalum body obtained by sintering Ta powder and a porous tantalum body covered with a Ta_2O_5 dielectric layer. Modeling showed a significant redistribution of contributions from pores of different types into the total capacitance after the formation of Ta_2O_5 due to the preferential isolation of the smallest pores and/or those difficult to access. The results of modeling of the frequency response of the analyzed samples agree well with the scanning electron microscopy data. The proposed approach has the potential to be advantageous for the technology of tantalum capacitors.

Keywords: Electrochemical impedance, Porous structure, Modeling

✉ Alexander V. Suygaev, e-mail: syual@udman.ru, syual@mail.ru

Condensed Matter and Interphases / Конденсированные среды и межфазные границы   2024;26(1): 135–145

A. V. Syugaev, V. E. Porsev   Electrochemical impedance of porous tantalum solids: modeling of frequency...

1. Introduction

Tantalum capacitors belong to electrolytic capacitors and are widely used in practice. In such capacitors, a porous pellet of sintered tantalum powder covered with a thin insulating layer of amorphous tantalum oxide, Ta_2O_5, serves as an anode. The electrolyte can be either liquid or solid, and being made of MnO_2 or conductive polymer (poly(3,4-ethylenedioxythiophene) polystyrene sulfonate). Since the capacitance arises at the interfaces, greater surface area of the porous body and its accessibility to the electrolyte improves capacitance characteristics of tantalum capacitors. To further develop the production technology of tantalum capacitors, new approaches to the characterization of the porous body structure are needed.

Electrochemical impedance spectroscopy is an effective technique for studying the electrochemical behavior of porous materials in various electrochemical systems and devices [1]. The frequency response of three-dimensional porous electrodes differs significantly from the response of flat electrodes, which allows an analysis of geometric factors of the porous structure [1–7]. An alternative approach to the study of porous structures is BET analysis which is based on the measurement of adsorption isotherms of gas molecules. However, the penetration of gases and fluids into a porous body is different, especially in the cases of small pores and/or high fluid viscosity. Viscous fluids (concentrated solutions of manganese nitrate hydrates, solutions of poly(3,4-ethylenedioxythiophene) polystyrene sulfonate) are widely used to form solid electrolyte layer in the porous body of tantalum capacitors. As a consequence, the BET analysis may give overestimated results of the surface area available for the fluid. That is why the electrochemical impedance technique is still preferable for porous tantalum bodies, since it allows studying the interaction of the porous structure with the fluid used as an electrolyte.

This work focuses on modeling the frequency response of porous tantalum bodies via an equivalent circuit that takes into account the hierarchy of pores and the features of ion transport in them. Using the modeling results the contributions from different type pores to the total capacitance and AC frequencies for their activation were determined. Samples of porous bodies were analyzed both before and after the formation of a Ta_2O_5 dielectric layer on their surface.

2. Experimental: samples, techniques and data processing

Porous tantalum samples were prepared as rectangular parallelepipeds 4.45×3.10×1.46 mm in size (anodes for tantalum capacitors) with a welded tantalum current collector. Samples were obtained from tantalum powder TaK-80 (detailed information on its morphology and chemical composition can be found in [8]), which was sintered at 1,330 °C in a vacuum furnace. The density of the samples after sintering was 5.0 g/cm³, which was much smaller than that of tantalum (16.65 g/cm³) and indicated their high porosity. Hereinafter, this sample will be referred to as *Ta*. Both as-sintered samples and samples with a grown Ta_2O_5 dielectric layer (~100 nm) formed by electrochemical oxidation in an aqueous solution of H_3PO_4 were analyzed. Hereinafter, the later is referred to as *Ta/Ta₂O₅*. The morphology of samples was studied with a Thermo Fisher Scientific Quattro S scanning electron microscope.

Electrochemical impedance was measured on a P-45X potentiostat with a built-in impedance measurement module (Electrochemical Instruments, Chernogolovka). The electrolyte was an aqueous solution of sodium sulphate with a concentration of 1 mol/l, deaerated with high-purity argon. To provide high-quality penetration of the electrolyte into the entire pore space, the samples were kept in the electrolyte for 16 hours. Measurements were taken in a glass cell with separated spaces for the working, auxiliary (Pt), and reference electrodes (Ag/AgCl). The distance between the sample and the Luggin capillary was 1 mm. The current collectors were insulated with paraffin.

Electrochemical impedance spectra were measured at potentials 100 mV higher than the open-circuit potentials ($E_{o.c.}$ = −215 mV for *Ta*; 635 mV for *Ta/Ta₂O₅* rel. Ag/AgCl electrode) to exclude the reduction reactions at the interface. Comparison of the porous structure relaxation of samples significantly different in structure is best done by analyzing the spectra measured at ~$E_{o.c.}$. It was difficult to apply the same potential for both samples, since a significant potential

Condensed Matter and Interphases / Конденсированные среды и межфазные границы   2024;26(1): 135–145

A. V. Syugaev, V. E. Porsev   Electrochemical impedance of porous tantalum solids: modeling of frequency...

shift from $E_{o.c}$ led to intensive side processes, which strongly affected the impedance spectra. For example, sample *Ta* at 600 mV relative to Ag/AgCl started to strongly oxidize. For sample Ta/Ta_2O_5, polarization at negative potentials caused transformations in the surface oxide layer.

Before measuring the spectra, the samples were kept for 45 min at a given potential to provide a steady state of the system. When measuring the spectra, the potential changed with the amplitude of ±5 mV and the frequency was ranged from 50 kHz to 10 mHz. Experimental data modeling was performed using the ZView software.

Capacitance characteristics of the samples are determined as follows [9, 10]. The impedance (Z) and capacitance (C) of the capacitor are related by the equation:

$$Z(\omega) = \frac{1}{j\omega C(\omega)},\tag{1}$$

where ω is the angular frequency and j is the imaginary unit.

The impedance can also be expressed in a complex form:

$$Z(\omega) = Z'(\omega) + jZ''(\omega),\tag{2}$$

where Z' and Z'' are the real and imaginary parts of impedance, respectively.

It follows from equations (1) and (2), that

$$C(\omega) = \frac{1}{\omega(jZ'(\omega) - Z''(\omega))} = \frac{-(Z''(\omega) + jZ'(\omega))}{\omega|Z(\omega)|^2}.\tag{3}$$

Capacitance can also be described by the following equation:

$$C(\omega) = C'(\omega) + jC''(\omega),\tag{4}$$

where C' and C'' are the real and imaginary parts of the capacitance, respectively.

From (3) and (4) it follows that

$$C'(\omega) = \frac{-Z''(\omega)}{\omega|Z(\omega)|^2},\tag{5}$$

$$C''(\omega) = \frac{-Z'(\omega)}{\omega|Z(\omega)|^2},\tag{6}$$

The real part of the capacitance (C') is close to the real capacitance of samples, which is observed, for example, in direct-current capacitance measurements (voltammograms, galvanostatic charge-discharge). The imaginary part (C'') corresponds to the energy dissipation under irreversible processes [9].

All dependences are given relative to the frequency f (Hz) related to the angular frequency as follows:

$$\omega = 2\pi f.\tag{7}$$

When calculating the impedance modulus ($|Z|$) and the phase angle (φ), the following equations are used:

$$|Z(f)| = \sqrt{(Z'(f))^2 + (Z''(f))^2},\tag{8}$$

$$\varphi(f) = \text{arctg}\,\frac{Z''(f)}{Z'(f)}.\tag{9}$$

The modified phase angle corrected for the resistance Z' at $f \to \infty$ is also calculated by formula [11]:

$$\varphi(f)_m = \text{arctg}\,\frac{Z''(f)}{Z'(f) - Z'(f \to \infty)}.\tag{10}$$

The value of Z' at $f \to \infty$ is determined from the $Z'(Z'')$ relationships by extrapolating a linear section with a slope of ~45° to the Z' axis. The use of the modified phase angle allows one to avoid a distortion of the phase angle in the high-frequency range associated with increased electrical resistance of the samples and the electrolyte, and provides better description of the $\varphi(f)$ dependence in terms of the porous structure response.

3. Results and discussion
3.1. Electrochemical impedance and capacitance of porous tantalum bodies

Fig. 1 shows electron microscopic images of the sample cleavage surfaces. The porous structure of the samples is clearly visible. In sample *Ta*, pores with a size of 1–3 µm (a-c) of almost spherical shape and pores of irregular shape in the range of 0.1–1 µm (on average ~0.3 µm) are observed. Many finer pores with a size of less than 0.1 µm are also observed (b-d). The porous structure of the Ta/Ta_2O_5 sample is markedly different (e-g), which is due to a dielectric layer. The oxide layer is visible as a grey-coloured shell ~ 100 nm thick along the edges of the particles in elastically scattered electrons (h). Large pores in Ta/Ta_2O_5 are 0.7–2 µm in size (e, f). There are also small pores (0.2 µm) and even smaller ones (f and g).

Condensed Matter and Interphases / Конденсированные среды и межфазные границы   2024;26(1): 135–145

A. V. Syugaev, V. E. Porsev   Electrochemical impedance of porous tantalum solids: modeling of frequency...
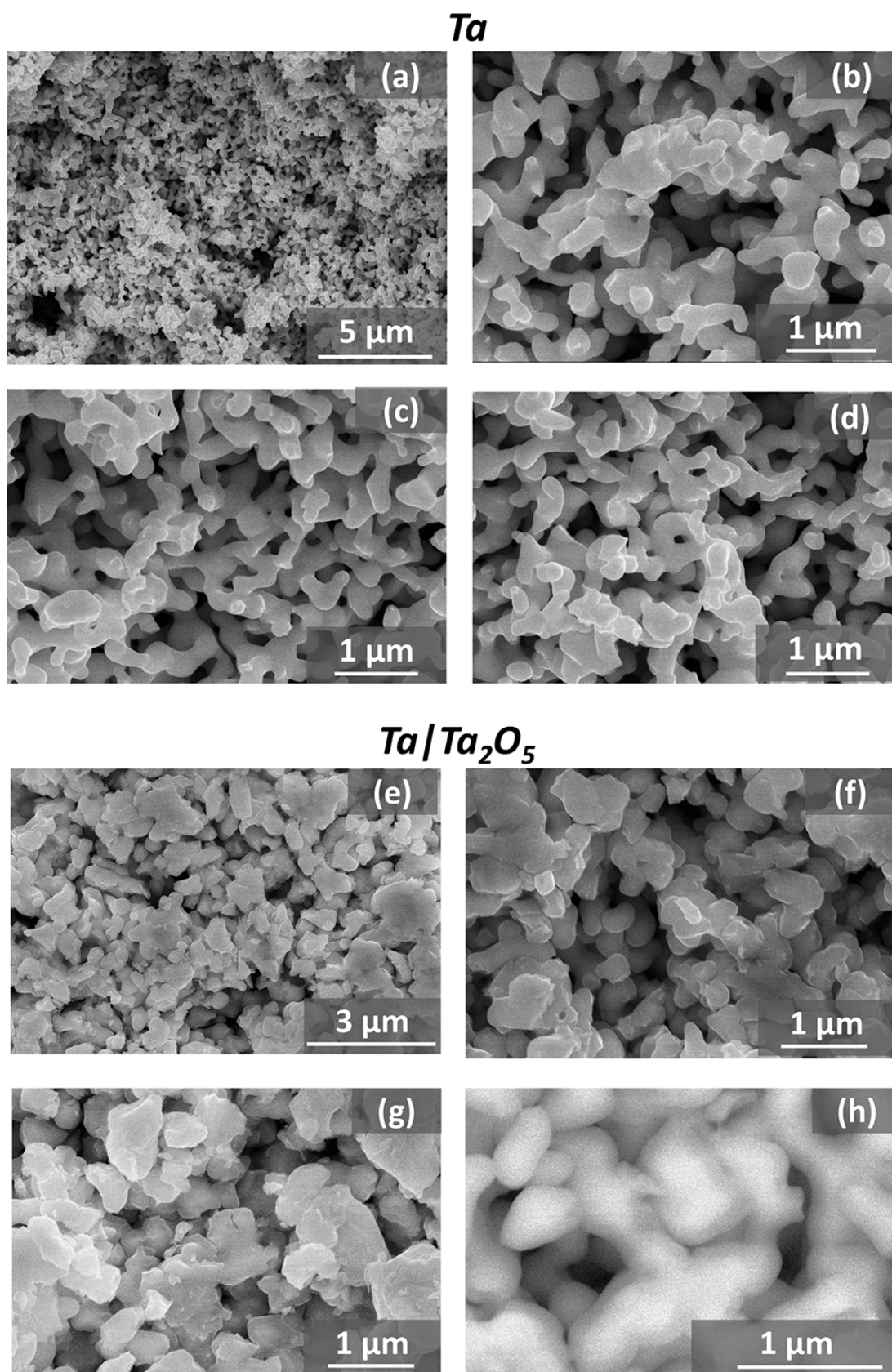
Ta

Ta|Ta₂O₅

Fig. 1. Electron microscopic images of *Ta* (a-d) and *Ta*/*Ta₂O₅* (e-h) cleavages in secondary (a-g) and in back-scattered electrons (h)

Condensed Matter and Interphases / Конденсированные среды и межфазные границы   2024;26(1): 135–145

A. V. Syugaev, V. E. Porsev   Electrochemical impedance of porous tantalum solids: modeling of frequency...

The dependences $Z'(Z'')$, $|Z|(f)$, and $\varphi(f)$ are shown in Fig. 2. For porous electrodes, the impedance phase angle is equal to half the phase shift angle for a smooth electrode with the same nature of interphase processes at $f\to\infty$ [1]. In the case of perfectly polarizable walls of a porous material, this should lead to the appearance at high frequencies of a characteristic section with a slope angle of ~45°, which becomes a vertical line. A similar shape of the impedance hodographs is observed for the studied porous tantalum bodies (see Fig. 2a, b).

The phase shift (Fig. 2c) for Ta and Ta/Ta_2O_5 at the high frequencies is in the range of −5 to −15°. Such value of φ is due to the phase shift distortion associated with the increased ESR (*Equivalent Series Resistance*) of the samples, which corresponds to Z' at $f\to\infty$ due to the electronic resistance of the contacts, the current collector, the material of the porous body, including the internal resistance of the particles and the resistance between the particles, as well as the ionic resistance of the electrolyte. The correction of the phase shift by the value of $Z'(f\to\infty)$ according to equation (10) gives the values of ~-45° at high frequencies (see the insert of Fig. 2c), which is most characteristic of porous electrodes [1–5].

The value of $Z'(f\to\infty)$ is significantly greater for Ta/Ta_2O_5 (6.7 Ω) as compared to the Ta sample (1.5 Ω). Since the same cell and electrolyte are used for the samples, the increase in $Z'(f\to\infty)$ corresponds to the increase in the electrical resistance of the porous body caused by the formation of the Ta_2O_5 dielectric layer. The Ta/Ta_2O_5 sample has significantly greater impedance over the entire AC frequency range (Fig. 2d).

At low frequencies, on $Z'(Z'')$ dependences, a line inclined relative to the Z' axis ($\varphi \sim -85°$) is observed instead of a vertical line ($\varphi = -90°$)

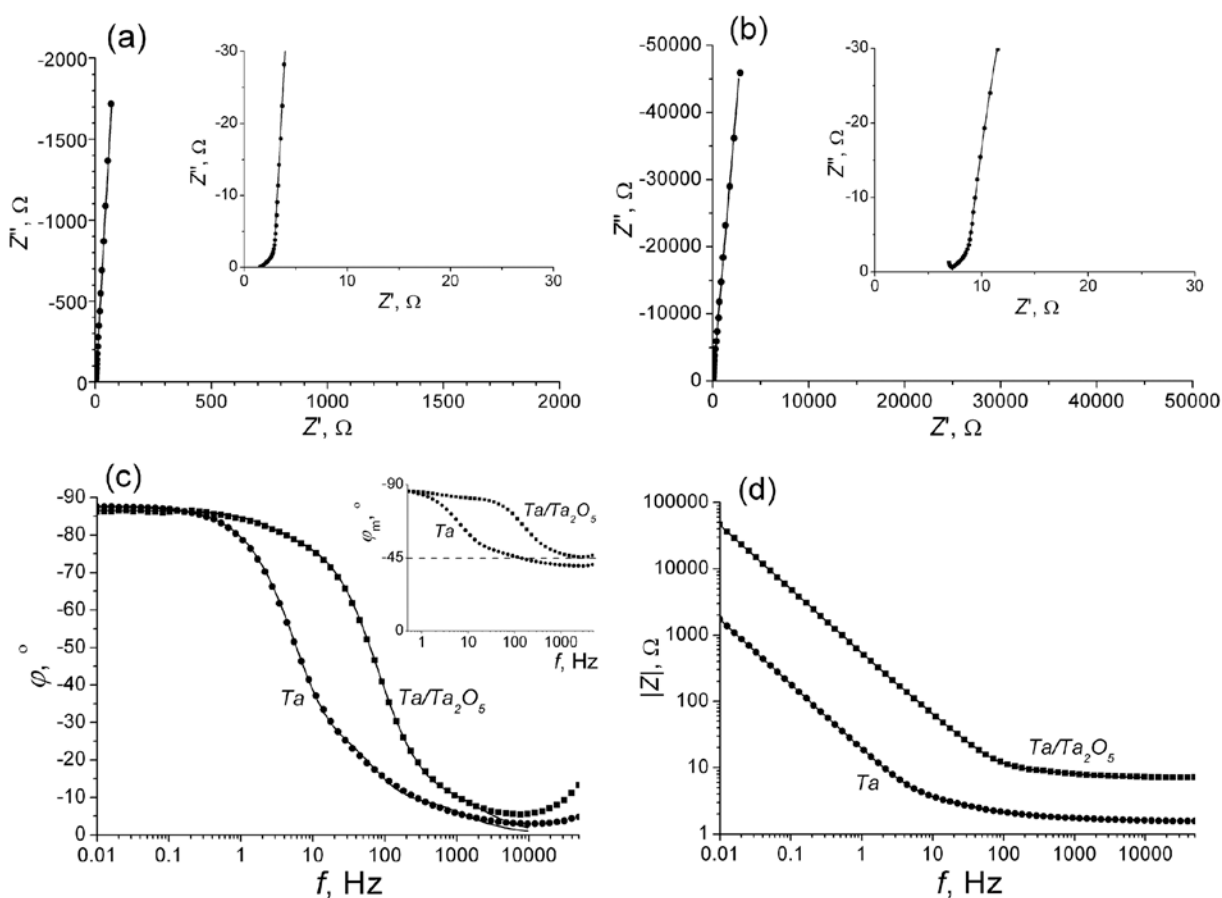**Fig. 2.** Nyquist plots for Ta (a) and Ta/Ta_2O_5 (b) samples; $\varphi(f)$ (c) and $|Z|(f)$ (d) dependences. The lines show the results of fitting using an equivalent circuit (see Section 3.2 for details). Inserts on (a) and (b) are the fragments of the Nyquist plots in the high-frequency region, an insert on (c) is the dependence of the phase shift vs. frequency, corrected according to equation (10)

Condensed Matter and Interphases / Конденсированные среды и межфазные границы   2024;26(1): 135–145

A. V. Syugaev, V. E. Porsev   Electrochemical impedance of porous tantalum solids: modeling of frequency...

characteristic of an ideal capacitor, which indicates non-ideal behavior modeled using the CPE element (*Constant Phase Element*). For an ideal capacitor, the impedance is:

$$Z_C = \frac{1}{j\omega C}, \tag{11}$$

For the CPE element, it is:

$$Z_{CPE} = \frac{1}{(j\omega)^\beta Q}, \tag{12}$$

where β is the ideality factor, usually located in the range of $0.9<\beta<1$ and Q is an imperfect capacitance ($F \cdot s^{\beta-1}$) [1]. Non-ideal behavior in the case of flat samples is usually due to the surface roughness [1, 12]. In the case of porous bodies, it can also be associated with the frequency response of the porous structure, depending on geometric factors and the pore size distribution [2, 3].

Higher frequency leads to deeper penetration of the AC signal into the pore and the gradual "activation" of the deeper walls of the pores [4, 13]. In an alternative approach which takes into account the pore size distribution, it is assumed that at the same frequency of alternating current, the depth of penetration into small pores is less than into large pores [2, 3]. At low enough frequencies, the entire surface of pores, including the smallest ones, contributes to interfacial impedance. Under these conditions, the impedance of the porous electrode becomes equal to the impedance of a flat electrode with a surface area equal to the total surface of the porous body.

Figure 3 shows the capacitance characteristics calculated from equations (5) and (6). The real part of the capacitance (C') is the closest to the real capacitance of the samples, which is observed,
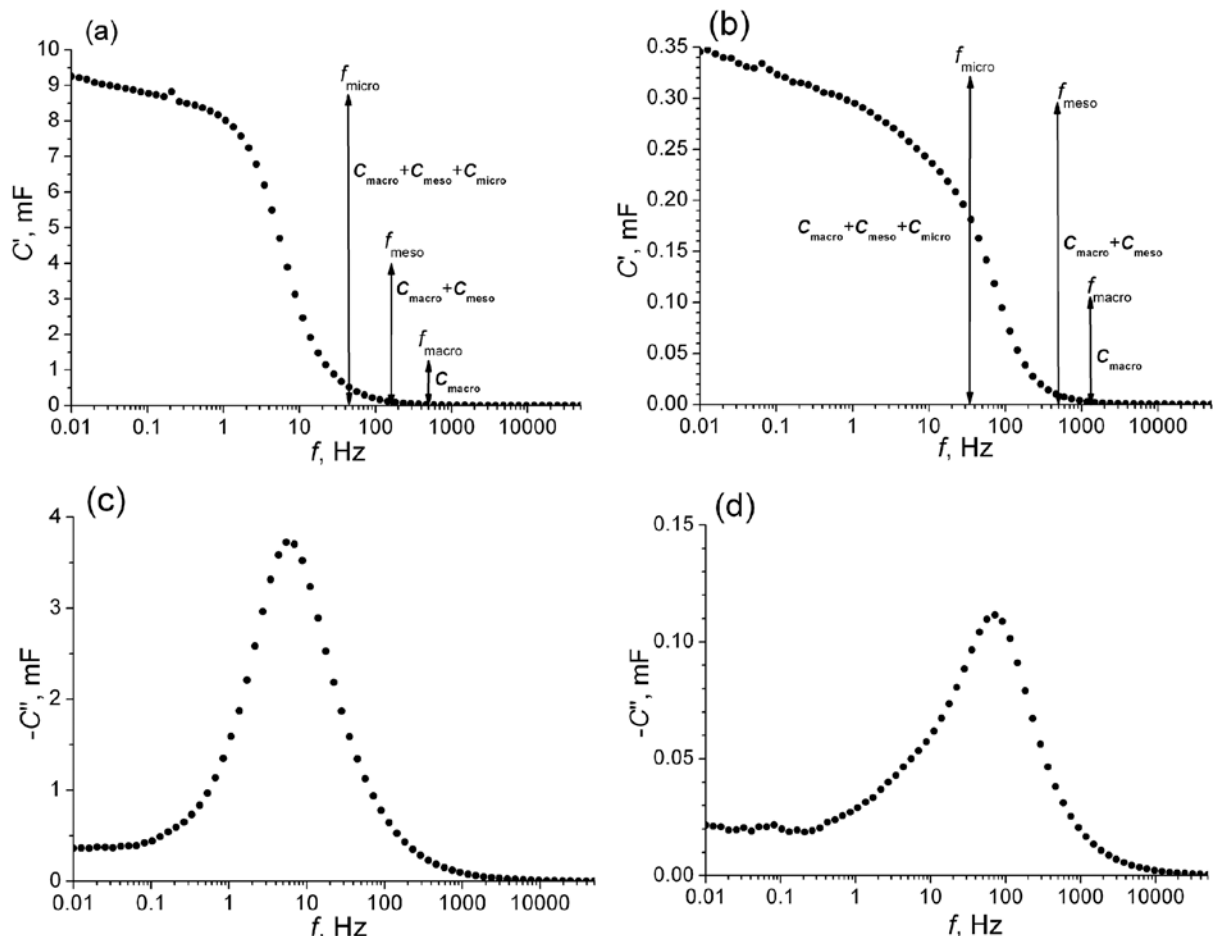

Fig. 3. Dependences of the real and imaginary part of the capacitance for *Ta* (a, c) and *Ta/Ta₂O₅* (b, d) on the AC frequency. The arrows in figures 3a and 3b additionally mark the activation frequencies of different types of pores and the capacitance per pores of different types, calculated from the modeling results using an equivalent circuit (see Section 3.2 for details)

Condensed Matter and Interphases / Конденсированные среды и межфазные границы   2024;26(1): 135–145

A. V. Syugaev, V. E. Porsev   Electrochemical impedance of porous tantalum solids: modeling of frequency...

for example, in direct current measurements (potentiodynamic voltammograms; galvanostatic charge-discharge) [9]. For the sample covered with a Ta_2O_5 layer, C' decreases significantly (~27 times at $f = 0.01$ Hz), which is associated with the appearance of a dielectric layer and a decrease in the surface area available for the electrolyte. Despite the different capacitance values, the $C'(f)$ relationship is similar for both samples, although the activation frequencies of C' were different.

The imaginary part C'' corresponds to the energy dissipation during irreversible processes [9]. For example, it could be heat losses associated with the rotation and movement of water molecules under the influence of alternating current, similar to heating in a microwave oven. It could also be losses associated with the redistribution of charges in the porous matrix [7]. $C''(f)$ dependences of the analyzed samples (Fig. 3c, d) are characterized by an extremum corresponding to the relaxation time of the entire system and the transition from the predominantly resistive to capacitive behavior of the samples [14]. The extremum on $C''(f)$ dependences is observed at a frequency at which φ = -45° (Fig. 2c).

3.2. Modeling the frequency response of porous tantalum bodies

In the case of porous tantalum bodies, when constructing an equivalent electrical circuit, it is necessary to take into account various elements that contribute to the overall resistance of the system: the resistance of the material itself, both between individual tantalum particles and within individual particles; the contact resistance between the current collector and the porous body; the resistance of the surface oxide; the ionic resistance of the electrolyte, consisting of the "external" surface resistance at the interphase boundaries, as well as the "internal" resistance of the electrolyte inside the pores of various sizes. The contribution of the charge transfer resistance in the case of Faradaic processes is also possible. The selection of a suitable transmission line modeling the frequency response of the porous structure is of key importance. At the moment, there are a number of approaches to modeling the frequency response of porous bodies, for example described in [2–6, 13, 15, 16]. The main approaches to the analysis of the electrochemical

impedance of porous electrodes were considered in one of the latest reviews [17].

One of the recent papers [7] proposed an interesting approach to modeling the behavior of porous carbon materials which took into account the pore hierarchy. The authors of that study compared the modeling results with BET analysis and mercury porosimetry data. It was assumed that electrolyte ions first penetrate into the larger pores (macropores), then into medium-sized pores (mesopores), and finally reach the smaller pores (micropores). This is schematically illustrated in Fig. 4a. The figure also demonstrates the difference in alternating current frequencies corresponding to the activation of pores of different types. This should lead to a deviation of the frequency response of the porous structure from the behavior of the ideal capacitor and should be taken into account when constructing an equivalent circuit. In the equivalent circuit proposed in [7] (Fig. 4b), the inductance element (L) modeled electrical contacts; the ESR referred mainly to the resistance of the electrolyte and the material itself. Then, R_{CT} is the charge transfer resistance with the constant phase element (CPE_{CT}) connected in parallel to take into account possible Faradaic processes at the interphase boundaries. Also, there is a short transmission line modeling the frequency response of the hierarchical porous structure. The focus is on determining the relaxation times ($RCPE$) for each pore type modeling the migration of ions through a hierarchical porous structure and related to their sizes. The sizes of macropores (> 50 nm), mesopores (2–50 nm), and micropores (< 2 nm) in [7] match those used in the standard classification of pore sizes. This circuit is successfully used to describe the electrochemical impedance of a series of carbon samples with different porosities obtained by cellulose pyrolysis. This approach also appears to be informative when analyzing the frequency response of porous samples of laser-induced graphene [18].

In this paper, an equivalent circuit is used, similar to that proposed in [7]. However, it has been modified. Charge transfer elements have been eliminated from the circuit. Since tantalum is an inert corrosion-resistant metal, the contribution of Faradaic processes to interfacial impedance and capacitance can be neglected under
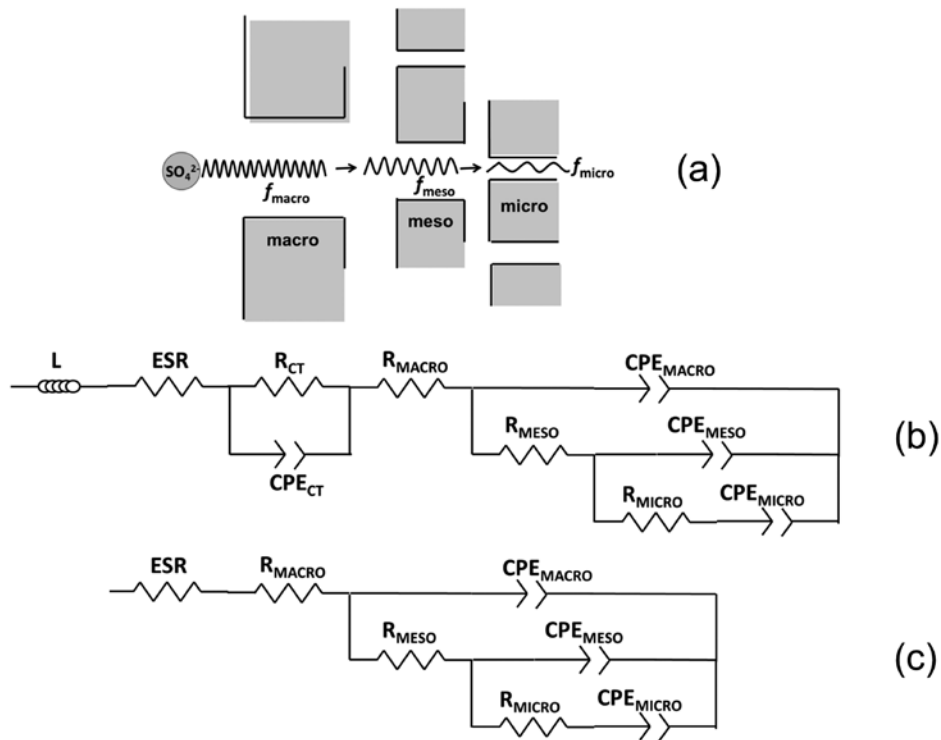
Condensed Matter and Interphases / Конденсированные среды и межфазные границы   2024;26(1): 135–145

A. V. Syugaev, V. E. Porsev   Electrochemical impedance of porous tantalum solids: modeling of frequency...

Fig. 4. Diagram demonstrating electrolyte transport in a porous structure, where ions move from macropores to mesopores, after which they enter micropores (a); equivalent circuit, modeling the frequency response of a hierarchical porous structure from [7] (b); modified equivalent circuit used to model the frequency response of porous tantalum bodies (c)

experimental conditions. The *L* element has also been eliminated, since in our case no inductance is observed in the high-frequency region, but it may be needed when measuring under other conditions, for example, with another electrolyte or in the AC frequency range. The modified circuit is shown in Fig. 4c. In the proposed circuit, the used designations of pores (macro-, meso-, and micro-) are just conventional names not related to the generally accepted classification of pores by size but only indicate their position in the hierarchy (Fig. 4a) and in the equivalent circuit (Fig. 4c). Relaxation times (τ) for each pore type were calculated as follows [7]:

$$\tau_{macro} = CPE_{macro}(ESR + R_{macro}), \tag{13}$$

$$\tau_{meso} = CPE_{meso}(ESR + R_{macro} + R_{meso}), \tag{14}$$

$$\tau_{micro} = CPE_{micro}(ESR + R_{macro} + R_{meso} + R_{micro}), \tag{15}$$

where *CPE* is non-ideal capacitance.

Fitting the electrochemical impedance spectra using a modified equivalent circuit (in the range of 0.01–10000 Hz) demonstrates good results: $\chi^2 = 0.00070071$ for *Ta* and $\chi^2 = 0.00080137$ for

Ta/Ta$_2$O$_5$. The fitting results are shown with solid lines in Fig. 2, with the main parameters given in Table 1 for the elements. Table 1 shows the total resistance for *ESR* and R_{macro} since it is not possible to separate their contributions in series circuits. For the *Ta/Ta$_2$O$_5$* porous body, all resistive elements in the circuit exhibit greater resistance as compared to *Ta*, which was associated with

Table 1. The main parameters of the equivalent circuit elements determined by fitting the experimental results

Element	*Ta*	*Ta/Ta$_2$O$_5$*
ESR+R_{macro}, Ω	1.621	7.212
$Q(CPE_{macro})$, mF·s$^{\beta-1}$	1.233	0.105
β_{macro}	0.93	0.96
R_{meso}, Ω	0.603	3.515
$Q(CPE_{macro})$, mF·s$^{\beta-1}$	2.745	0.186
β_{meso}	0.99	0.96
R_{micro}, Ω	2.604	1074
$Q(CPE_{macro})$, mF·s$^{\beta-1}$	4.719	0.027
β_{micro}	0.98	1.01

Condensed Matter and Interphases / Конденсированные среды и межфазные границы   2024;26(1): 135–145

A. V. Syugaev, V. E. Porsev   Electrochemical impedance of porous tantalum solids: modeling of frequency...

a dielectric layer and an increase in electrolyte resistance with decreasing pore sizes [15]. While (ESR+R_{macro}) and R_{meso} increased 4–6 times, R_{micro} increases ~400 times, i.e. the most significant changes are due to pores of smaller size difficult to access.

The obtained modeling results provide additional data on the behavior of the porous structure, not available in [7]. Since factor β for CPE elements varies from 0.93 to 1.01 which means low deviation from the ideal capacitance for pores of any type, the non-ideal CPE capacitance (Q) may be considered as the ideal capacitance (C) for each type of pores. This is supported by the fact that the sum of capacitances ($\sum C$) for all types of pores determined from the model agreed well with the values of C' (at a minimum frequency of f = 0.01 Hz) obtained in the experiment. For the Ta sample, $\sum C$ = 8.70 mF, $C'(0.01)$ = 9.26 mF, the difference was only 6%. For Ta/Ta_2O_5, $\sum C$ = 0.318 mF, $C'(0.01)$ = 0.345 mF, the difference was 8%.

In this paper, we also determined frequencies of the activation onset (activation frequencies) of each pore type based on the calculated relaxation time, which corresponded to the transition from predominantly resistive to capacitive behavior. The activation frequency was determined as follows:

$$f_{pore} = \frac{1}{\tau_{pore}}. \qquad (16)$$

Table 2 shows the fractions of the capacitance attributable to each type of pores, as well as the relaxation times and activation frequencies of different type pores, determined from equations (13)–(16). For clarity, the activation frequencies and the fraction of the capacitance for different types of pores obtained by modeling of the frequency response are shown by the arrows on the C'-f dependences (Fig. 3a and b).

Relatively low relaxation times indicate that the majority of pores according to the standard classification are macropores (> 50 nm). For example, the relaxation time for macropores in [7] is on the order of ten milliseconds. As mentioned above, the used classification of pores is based on their position in the hierarchy (Fig. 4a). The hierarchy of the porous structure is clearly observed in electron microscopic images (Fig. 1).

For the Ta sample, the "macropores" contributing 14% of the capacitance are most likely pores 1–3 μm in size (Fig. 1a-c). "Mesopores" making 32% of the capacitance are 0.1–1 μm in size, with the average size of ~0.3 μm (Fig. 1b-c). More than half of the capacitance arises from "micropores" with a size of ⩽0.1 μm (Fig. 1b-c). The ratio of capacitance fractions from "macropores" and "mesopores" is approximately 1 to 2, being comparable for Ta and Ta/Ta_2O_5. The dimensions of "macropores" (0.7–2) and "mesopores" (⩽0.2 μm) for Ta/Ta_2O_5 are smaller (Fig. 1d-f) than for Ta, which is associated with the appearance of a 100 nm thick oxide layer in them. There is a sharp decrease in the contribution from the "micropores" from 54 to 9% on going from the Ta sample to the Ta/Ta_2O_5 sample. This is due to the fact that "micropores" are blocked by the oxide layer, since the dimensions of "micropores" in Ta are comparable to the thickness of the dielectric layer in Ta/Ta_2O_5. However, they are not blocked completely. It is difficult to observe "micropores" in electron microscopic images for Ta/Ta_2O_5 because of their small size and low amount.

Relaxation times can be used to compare pore sizes in samples with similar pore shapes, interphase boundaries, and processes. Provided that all other conditions are equal, the smaller the pore size, the longer the relaxation time and the lower its activation frequency [2, 3, 7]. Due to the difference in the thickness of oxide layers in Ta and Ta/Ta_2O_5, it is impossible to compare the pore sizes in these samples based

Table 2. Capacitance fractions, characteristic relaxation times, and activation frequencies for pores of different type calculated from the parameters of the circuit modeling the frequency response of a porous body

	«Macropores»			«Mesopores»			«Micropores»		
	N, %	τ_{macro}, ms	f_{macro}, Hz	N, %	τ_{meso}, ms	f_{meso}, Hz	N, %	τ_{micro}, ms	f_{micro}, Hz
Ta	14	2.00	500	32	6.10	164	54	22.8	44
Ta/Ta_2O_5	33	0.76	1316	58	2.00	500	9	29.3	34

Condensed Matter and Interphases / Конденсированные среды и межфазные границы   2024;26(1): 135–145

A. V. Syugaev, V. E. Porsev   Electrochemical impedance of porous tantalum solids: modeling of frequency...

on the calculated relaxation times. The oxide layer of large thickness leads to a decrease in the relaxation times of "macro-" and "mesopores" in the case of Ta/Ta_2O_5 as compared to Ta despite the reduction in their sizes. On the other hand, a longer "micropore" relaxation time for Ta/Ta_2O_5 as compared to Ta may indicate a particularly significant decrease in their size in Ta/Ta_2O_5.

4. Conclusions

It has been shown that using an equivalent circuit that takes into account the hierarchy of pores in the porous body allows one to describe the electrochemical impedance of porous tantalum bodies. It can also provide valuable information about the features of the porous structure and its interaction with the liquid phase. The results obtained by modeling the frequency response of real samples agree well with the data obtained by scanning electron microscopy. The proposed approach to modeling the impedance spectra makes it possible to estimate the accessibility of the porous structure for the electrolyte and to determine the fraction of the surface related to each type of pores. These data can be useful for determining the characteristics of a porous structure depending on the modes of preparing and treatment of a porous body in the tantalum capacitors technology. It is also possible to model the interaction of the porous structure of tantalum bodies with fluids used to prepare solid electrolytes of tantalum capacitors (concentrated solutions of manganese nitrate, solutions of poly(3,4-ethylenedioxythiophene) polystyrene sulfonate).

Author contributions

A. V. Sugaev: research concept, methodology development, conducting research, text writing, final conclusions. V. E. Porsev: conducting research, writing and editing the text.

Conflict of interests

The authors declare that they have no known competing financial interests or personal relationships that could have influenced the work reported in this paper.

References

1. Kichigin V. I., Sherstobitova I. N., Shein A. B. *Impedance of electrochemical and corrosion systems: textbook*.* Perm State University Publ.; 2009. 238 p. (In Russ.)

2. Song H.-K., Jung Y.-H., Lee K.-H., Dao L. H. Electrochemical impedance spectroscopy of porous electrodes: the effect of pore size distribution. *Electrochimica Acta.* 1999;44(20): 3513–3519. https://doi.org/10.1016/S0013-4686(99)00121-8

3. Song H.-K., Hwang H.-Y., Lee K.-H., Dao L. H. The effect of pore size distribution on the frequency dispersion of porous electrodes. *Electrochimica Acta.* 2000;45(14): 2241–2257. https://doi.org/10.1016/S0013-4686(99)00436-3

4. Keiser H., Beccu K. D., Gutjahr M. A. Abschätzung der porenstruktur poröser elektroden aus impedanzmessungen. *Electrochimica Acta.* 1976;21(8): 539–543. https://doi.org/10.1016/0013-4686(76)85147-X

5. Candy J.-P., Fouilloux P., Keddam M., Takenouti H. The characterization of porous electrodes by impedance measurements. *Electrochimica Acta.* 1981;26(8): 1029–1034. https://doi.org/10.1016/0013-4686(81)85072-4

6. Raistrick I. D. Impedance studies of porous electrodes. *Electrochimica Acta.* 1990;35(10): 1579–1586. https://doi.org/10.1016/0013-4686(90)80013-E

7. Abouelamaiem D. I., He G., Neville T. P., ... Brett D. J. L. Correlating electrochemical impedance with hierarchical structure for porous carbon-based supercapacitors using a truncated transmission line model. *Electrochimica Acta.* 2018;284: 597–608. https://doi.org/10.1016/j.electacta.2018.07.190

8. Treshchev S. Yu., Starostin S. P., Mikhailiva S. S., ...Lebedev S. P. Comparative analysis of the composition and structure of condenser tantalum powder. *Chemical Physics and Mesoscopy.* 2014;16(4): 609–615. (In Russ., abstract in Eng.). Available at: https://www.elibrary.ru/item.asp?id=22662614

9. Taberna P. L., Simon P., Fauvarque J. F. Electrochemical characteristics and impedance spectroscopy studies of carbon-carbon supercapacitors. *Journal of The Electrochemical Society.* 2003;150(3): A292–A300. https://doi.org/10.1149/1.1543948

10. Itagaki M., Suzuki S., Shitanda I., Watanabe K. Electrochemical impedance and complex capacitance to interpret electrochemical capacitor. *Electrochemistry.* 2007;75(8): 649–655. https://doi.org/10.5796/electrochemistry.75.649

11. Orazem M. E., Pébère N., Tribollet B. Enhanced graphical representation of electrochemical impedance data. *Journal of The Electrochemical Society.* 2006;153(4): B129–B136. https://doi.org/10.1149/1.2168377

12. Pajkossy T. Impedance spectroscopy at interfaces of metals and aqueous solutions – Surface roughness, CPE and related issues. *Solid State Ionics.* 2005;176(25-28): 1997–2003. https://doi.org/10.1016/j.ssi.2004.06.023

Condensed Matter and Interphases / Конденсированные среды и межфазные границы   2024;26(1): 135–145

A. V. Syugaev, V. E. Porsev   Electrochemical impedance of porous tantalum solids: modeling of frequency...

13. Macdonald D. D., Urquidi-Macdonald M., Bhakta S. D., Pound B. G. The electrochemical impedance of porous nickel electrodes in alkaline media: II. Nonuniform transmission line analysis. *Journal of The Electrochemical Society*. 1991;138: 1359–1363. https://doi.org/10.1149/1.2085786

14. Lima-Tenório M. K., Ferreira C. S., Rebelo Q. H. F., ... Aparecido Pocrifka L. Pseudocapacitance properties of Co_3O_4 nanoparticles synthesized using a modified sol-gel method. *Materials Research*. 2018;21(2): e20170521. https://doi.org/10.1590/1980-5373-mr-2017-0521

15. Nquyen P. H., Paasch G. Transfer matrix method for the electrochemical impedance of inhomogeneous porous electrodes and membranes. *Journal of Electroanalytical Chemistry*. 1999;460(1-2): 63–79. https://doi.org/10.1016/S0022-0728(98)00343-X

16. Conway B. E. *Electrochemical supercapacitors: scientific fundamentals and technological applications*. Springer Science & Business Media; 2013. 607 p.

17. Huang J., Gao Y., Luo J., ... Zhang J. Editors' choice—review—impedance response of porous electrodes: theoretical framework, physical models and applications.. *Journal of The Electrochemical Society*. 2020;167: 166503. https://doi.org/10.1149/1945-7111/abc655

18. Syugaev A. V., Zonov R. G., Mikheev K. G., Maratkanova A. N., Mikheev G. M. Electrochemical impedance of laser-induced graphene: Frequency response of porous structure. *Journal of Physics and Chemistry of Solids*. 2023;188: 111533. https://doi.org/10.1016/j.jpcs.2023.111533

Information about the authors

Alexander V. Syugaev, Cand. Sci. (Chem.), Research Fellow at the Laboratory of Ultrafine Systems, Department of Physics and Chemistry of Nanomaterials of Physical-Technical Institute, Udmurt Federal Research Center (Izhevsk, Russian Federation).

https://orcid.org/0000-0002-2190-395X
syual@udman.ru

Vitaly E. Porsev, Cand. Sci. (Phys.-math), Leading Research Fellow at the Laboratory of Mechanical Activation of Organic Systems, Department of Physics and Chemistry of Nanomaterials of Physical-Technical Institute, Udmurt Federal Research Center (Izhevsk, Russian Federation).

https://orcid.org/0000-0003-1949-7371
porsev@udman.ru